INTERNATIONAL JOURNAL of PARTICLE THERAPY

Monte Carlo Simulations of Neutron Ambient Dose Equivalent in a Novel Proton Therapy Facility Design

Uwe Titt, PhD; Enzo Pera, MEE; Michael T. Gillin, PhD

University of Texas, M. D. Anderson Cancer Center, Houston, TX, USA

Abstract

Purpose: The neutron shielding properties of the concrete structures of a proposed proton therapy facility were evaluated with help of the Monte Carlo technique. The planned facility's design omits the typical maze-structured entrances to the treatment rooms to facilitate more efficient access and, instead, proposes the use of massive concrete/steel doors. Furthermore, straight conduits in the treatment room walls were used in the design of the facility, necessitating a detailed investigation of the neutron radiation outside the rooms to determine if the design can be applied without violating existing radiation protection regulations. This study was performed to investigate whether the operation of a proton therapy unit using such a facility design will be in compliance with radiation protection requirements.

Methods: A detailed model of the planned proton therapy expansion project of the University of Texas, M. D. Anderson Cancer Center in Houston, Texas, was produced to simulate secondary neutron production from clinical proton beams using the MCNPX Monte Carlo radiation transport code. Neutron spectral fluences were collected at locations of interest and converted to ambient dose equivalents using an in-house code based on fluence to dose-conversion factors provided by the International Commission on Radiological Protection.

Results and Conclusions: At all investigated locations of interest, the ambient dose equivalent values were below the occupational dose limits and the dose limits for individual members of the public. The impact of straight conduits was negligible because their location and orientation were such that no line of sight to the neutron sources (ie, the isocenter locations) was established. Finally, the treatment room doors were specially designed to provide spatial efficiency and, compared with traditional maze designs, showed that while it would be possible to achieve a lower neutron ambient dose equivalent with a maze, the increased spatial (and financial) requirements may offset this advantage.

Keywords: neutron shielding; proton therapy; Monte Carlo study

Submitted 23 July 2019
Accepted 22 Jan 2020
Published 12 Mar 2020

Corresponding Author:
Uwe Titt
Department of Radiation Physics
University of Texas M. D. Anderson Cancer Center
Pickens Academic Tower
1400 Pressler Street, Unit 1420
Houston, TX 77030-3722, USA
Phone: +1 (713) 563-2558
utitt@mdanderson.org

Original Article

DOI
10.14338/IJPT-19-00071.1

http://theijpt.org

Introduction

The erection of a new proton therapy facility warrants a thorough investigation of the shielding against unwanted exposure of workers and members of the public inside and outside the facility. In a proton therapy facility, the nuclei of hydrogen (protons) are accelerated to kinetic energies up to 230 MeV to allow the particles to penetrate deep into a patient's tissue and reach the target volume to sterilize cancer cells. However, not

all protons that are being accelerated reach the target; a sizable fraction collides with various materials of the accelerator and the beam transport system. All of the protons that are colliding with matter have a finite probability to interact with molecules of the material they traverse. Finally, the protons that reach the target react with the molecules of the patient's tissue. The 2 main reaction channels open to protons traversing matter are ionization and, to a smaller degree, nuclear reactions. Nuclear reactions may be further distinguished into elastic and inelastic reactions. Inelastic nuclear reactions are again divided into direct reactions, when a primary proton directly knocks out 1 or more particles from the target nucleus, and indirect reactions, where the proton is absorbed by a target nucleus that subsequently emits 1 or more particles from the so-called compound nucleus. Direct and indirect inelastic reactions of protons in any material lead to the emission of secondary neutrons (and to a lesser degree other charged particles, such as secondary protons, alphas, or heavier fragments of the target nuclei). Neutrons are known to be a health hazard, having a large relative biological effectiveness [1, 2], and because of their charge neutrality they are notoriously difficult to control. The main method to reduce the risk of neutron exposure is to slow the neutrons down to thermal energies and allow them to be absorbed by nuclei in the shielding material (eg, concrete, iron, steel). The most efficient energy transfer takes place between neutrons and light nuclei, which makes concrete an efficient radiation barrier because of the its relatively high content of hydrogen and oxygen. Another possibility is that the neutrons undergo neutron-β-decay into a proton, an electron, and an electron-neutrino; however, the half-life of a free neutron is on the order of 10 minutes and, hence, this channel is unlikely to play a significant role in the context of radiation protection in a proton therapy facility.

Because measurements can only be performed in existing facilities, the neutron exposure in a planned facility must be estimated by means of analytical calculations, which provide rough estimates in a short amount of time, or with Monte Carlo simulations, which provide more accurate results but need significantly more computation time. Several planned and existing ion therapy facilities have been simulated with Monte Carlo [3–13], and comparison of the simulation results with analytical estimates and measured values have shown to provide conservative estimates of actual (measured) secondary neutron exposure.

This study describes the Monte Carlo simulations of secondary neutron dose in a newly planned proton therapy facility in Houston, Texas. The purpose of this study is to verify that the shielding design performs adequately and that the dose to individual members of the public and occupational doses will comply with the radiation protection limits as defined in the Texas Administrative Code [14]. These limits are an annual occupational dose of 50 mSv and the dose limits for individual members of the public are defined as doses not exceeding 5 mSv annually and a dose not exceeding 0.02 mSv in any 1 hour.

Particular attention was paid to the overall impact of conduits, including traditionally designed conduits, with a double bend and to straight conduits in the treatment room walls. The differences in ambient neutron dose equivalent values was evaluated by simulating the facility with and without the conduits in place.

Finally, the impact of the treatment room doors was assessed because of the novel design using sliding doors instead of the maze concept. Ambient neutron dose values in locations near the sliding doors were compared with data from treatment-room exit designs using traditional mazes of typical dimensions.

Methods and Materials

A detailed Monte Carlo model of the facility building was created using MCNPX 2.7.0 [15] based on the vendor's blueprints (Hitachi, Ltd, Tokyo Japan). The model comprised the concrete structure, selected shielding elements (eg, additional metal plates near the particle accelerator and inside the treatment rooms), and beam line elements where accelerated protons can collide with the equipment and produce secondary radiation, mostly neutrons. **Figure 1** shows a schematic drawing of the cross section of the facility, including some relevant receptor locations. The concrete composition, listed in **Table 1**, was based on a mixture commonly known as "Portland concrete" [16, 17], with a density of 2.35 g/cm^{-3}. Some locations (the outside walls close to the accelerator) were modeled with a high-density concrete [17], the composition of which is also shown in **Table 1**. The density of this material was assumed to be 3.4 g/cm^{-3}. **Figure 1** also shows details of the sliding door in a top-down view. The distance between the walls and the door was 9.4 cm, and the gap to the floor was about 1.2 cm. The materials of the door was 61 cm of concrete sandwiched between 2 steel plates of 7.62 cm in thickness each. In addition, **Figure 1** shows 2 maze designs evaluated in this study.

The materials and densities for the proton targets were chosen according to the vendor's specification of the respective device where beam may be lost during operation. The targets in the treatment rooms, representing patients, were modeled of water. All targets' sizes were determined by the stopping lengths [18] of the simulated proton beams.

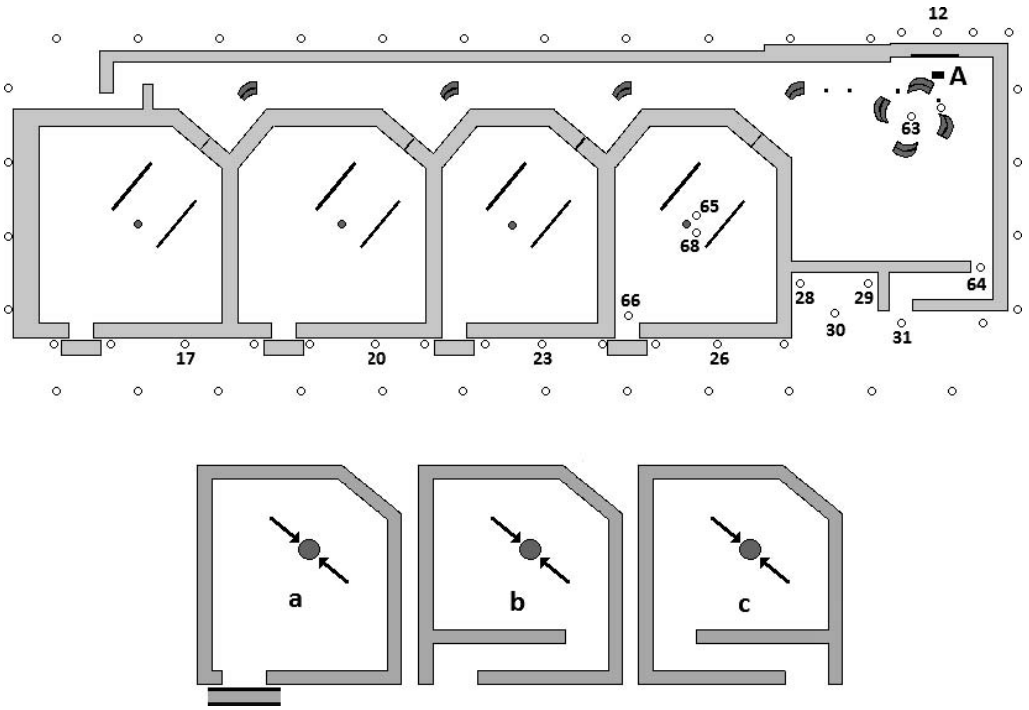

Figure 1. The facility layout of the Monte Carlo model, including some relevant neutron spectral fluence receptor locations. Receptors 17, 20, 23, and 26 are located in the treatment control rooms, and receptors 28, 29, and 30 are located in the main control room. Additional local shielding was modeled at location **A**. The lower image depicts a schematic top-down view of the treatment room door designs showing the sandwich design and the 9.4-cm air gap between the door and the walls of the sliding door (a) and the more traditional maze designs (b and c). The filled circles are the isocenter location in the rooms, and the arrows indicate 2 out of 4 simulated proton beam directions. The remaining 2 are normal and antinormal to the image plane.

The radiation transport simulations through these models were facilitated as follows. Proton beams of different kinetic energies (50, 170, 200, and 230 MeV) were simulated impinging on the targets. The neutron sources inside the accelerator magnets were approximated by multiple sources, and the extraction beam loss point at the proton beam extraction was approximated as a line source. Because of an expected high-dose region close to receptor No. 12, originating from high-energy protons colliding with a high-Z material of the extraction electrode of the accelerator, additional local shielding was implemented to achieve compliance with the radiation protection limits. At location A in **Figure 1**, a 20.3 cm (8 inch) thick ferrite slab was integrated into the concrete wall and an additional local concrete block 50-cm thick was located between the accelerator and the outside wall. Inside the treatment rooms, the proton beams for each energy were simulated at 4 cardinal angles around the rotational axis of the gantries.

Table 1. Portland concrete and high-density concrete composition.

Nuclide	Portland mass fraction (%)	High-density mass fraction (%)
H	1.00	0.44
C	0.10	0.04
O	52.91	31.26
Mg	0.20	0.39
Al	3.39	0.17
Si	33.7	0.19
Ca	4.40	4.36
K	1.30	0.06
Na	1.60	–
Fe	1.40	60.8
N	–	0.003
S	–	0.04
V	–	0.05
Mn	–	0.06
Ti	–	0.19
P	–	0.29

Table 2. Annual proton losses.

Loss point	Beam energy (MeV)	Charge lost (μC y^{-1})				
Injection	7	1980				
Synchrotron bending magnets	230	180				
	200	360				
	170	180				
	50	2760				
Total synchrotron bending magnets		3480				
Scraper	50	8868				
Beam extraction	230	80				
	200	164				
	170	80				
Fast Faraday cup	230	40				
	200	76				
	170	40				
Beam damper	230	68				
	200	136				
	170	68				
			Gantry angle (°)			
			0	90	180	270
Isocenter (each)	230	→	68	68	10	11
	200	→	137	130	19	21
	170	→	68	68	10	11

The particle transport in the Monte Carlo simulations was limited to protons and secondary neutrons. The Bertini physics model was selected for the simulation of intranuclear cascades, and in all material definitions the ENDF/B-VII cross-section data tables were used. The number of source particles was set to 5×10^8 and no variance reduction techniques were applied, resulting in an average cpu-time of 1.5×10^5 minutes for each simulation. Secondary neutron spectral fluence Φ, was scored in 69 spherical volumes, in the following referred to as "receptors." distributed throughout the facility. The receptors were defined with exponential binning from 0 MeV through 275 MeV, and the results were scored in units of cm^{-2} per source proton.

Two different conduit designs were used in the facility: 1 in the traditional shape with 2 bends and 1 straight through the wall. Both designs, each with a diameter of about 10 cm, were implemented in the model according to the original blueprints. By design, the straight conduits were located at a height ensuring that there was no line of sight through the conduits to the most prominent neutron source, that is, the isocenter in the treatment rooms. Last but not least, the air conditioning ducts were modeled similar to the traditional design (featuring two 90° bends) with a diameter of about 40 cm.

All scored neutron spectral fluences were summed, weighted with usage factors to estimate annual and hourly values. These usage factors consisted of conservatively estimated quantities of the charge lost at each beam loss location. The annual values applied in this study are shown in **Table 2**. Note that these values constitute the worst-case scenario, taking into account different usage patterns of the facility during commissioning and routine clinical use. Estimates of the hourly ambient neutron dose equivalent were based on the assumption of a full hour of beam on time with the highest available proton energy, corresponding to the highest neutron production probability.

The summed spectra were then converted to neutron ambient dose equivalent spectra by applying in-house code, calculating the fluence to dose conversion factors, h, in units of pSv/cm^{-2} from Petoussi-Henss and colleagues [19]. **Figure 2** shows a plot demonstrating the agreement between calculated values and the tabulated values from the International Commission on Radiological Protection.

The product of the weighted neutron spectral fluence Φ and the conversion factor h of each receptor was summed over all neutron energy bins and yielded the total ambient dose equivalent, $H^*(10) = \Sigma_{i=0}^{275MeV} \Phi \times h \times \Delta E_i$ in units of pSv at each receptor location. The width of each energy bin, i, is denoted by ΔE_i. This formalism follows the method described by Polf and colleagues [20]. The neutron ambient dose equivalent is an operational quantity based on dose equivalent and defined by the

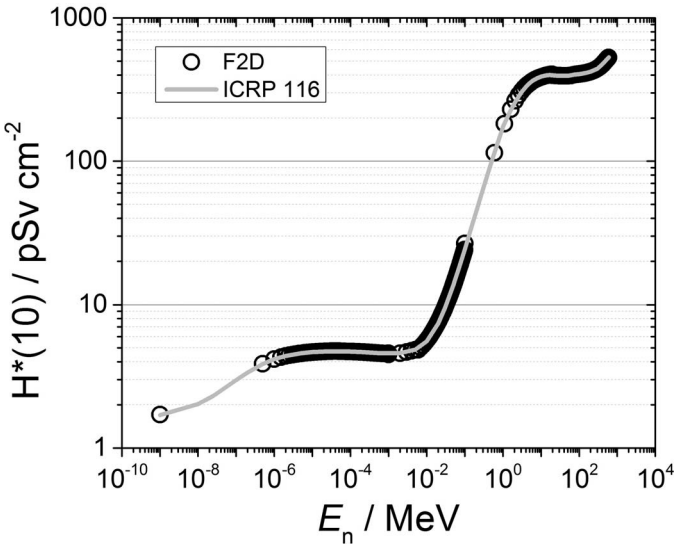

Figure 2. The fluence to dose conversion factor, *h*, in units of pSv cm^{-2}, taken from ICRP 116 [19] and from the in-house conversion code (F2D). The solid line shows the tabulated data from ICRP 116, and the scatterplot (circles) depicts values calculated with F2D. Note that thermal neutrons convert to rather small doses, and only neutrons with kinetic energies larger than about 100 keV contribute significantly to the ambient dose equivalent.

International Commission on Radiation Units [21] for measurements in external radiation fields. It provides a conservative estimate of equivalent dose, the protection quantity related to an exposure or potential exposure of persons under most irradiation conditions.

To assess the overall impact of the conduits on the ambient neutron dose equivalent, 2 simulations were performed. One simulation was performed in a model containing air-filled conduits as designed by the vendor, and 1e without the conduits in place. Differences in annual ambient neutron dose equivalent were then computed at all receptor locations.

The differences in shielding properties of the sliding-door design and the traditional maze designs were estimated by comparing the neutron fluence and the ambient dose equivalent outside the door. The maximum proton energy was simulated to provide a maximum neutron fluence inside the treatment room. The neutron ambient dose equivalent values scored in the maze-featuring runs were then compared with the sliding-door receptor. The maze's concrete wall inside the treatment room had a thickness of 115 cm, typical for this structure. For a proton energy of 230 MeV and for the 4 considered gantry angles (0°, 90°, 18°, 270°), an annual proton loss of 2.5×10^{14} was assumed. No self-shielding of the gantry was taken into account for these simulations to provide worst-case conditions; all rooms were empty, except for a water sphere of stopping-length size at the isocenter.

Results

A 2-dimensional plot of the weighted sum of the neutron fluence in the X-Y plane (at isocenter height, ie, 130 cm above the ground level) is shown in **Figure 3a**. The values are given on a logarithmic scale in arbitrary units spanning 10 orders of magnitude and are provided to demonstrate the integrity of the geometry and to show the relative intensity of total neutron fluence.

Examples of simulated neutron spectral fluences recorded at the center of the accelerator, at the entrance and exit of the maze to the accelerator room (see **Figure 1**, receptors 63, 64, and 31) are also shown in **Figure 3b** and **3c**.

The annual H*(10) values summed over all spectra are shown in **Figure 4a**. Finally, **Figure 4b** shows the hourly ambient dose equivalent, calculated by using beam loss weights, assuming a full hour of accelerator operation without interruption at the maximum beam energy (230 MeV). All receptors located in public areas showed values below the legal limits of 5 mSv per year and 0.02 mSv per hour. The receptors located in the occupational areas, including the main control room and the treatment control rooms, all showed annual ambient dose equivalent values below 13 mSv per year, which is a factor of about 4 below the legal limit of 50 mSv per year for occupational dose**. Figure 4a** and **4b** shows 2 data points named "TXroom" and "outside alignment hole," which were used to assess the impact of holes in the concrete walls, which would be bored into the wall at the time of construction to facilitate accurate alignment of the beam-line equipment. The former refers to a receptor in the rightmost treatment room next to the accelerator room. The receptor was located at the exit of the alignment hole. The hole in the model was simulated to contain relatively low-density steel (approximating steel wool) and to be sealed with steel disks of 2.54-cm thickness. The exposure of this receptor was evaluated with weights rearranged such that the beam was directed

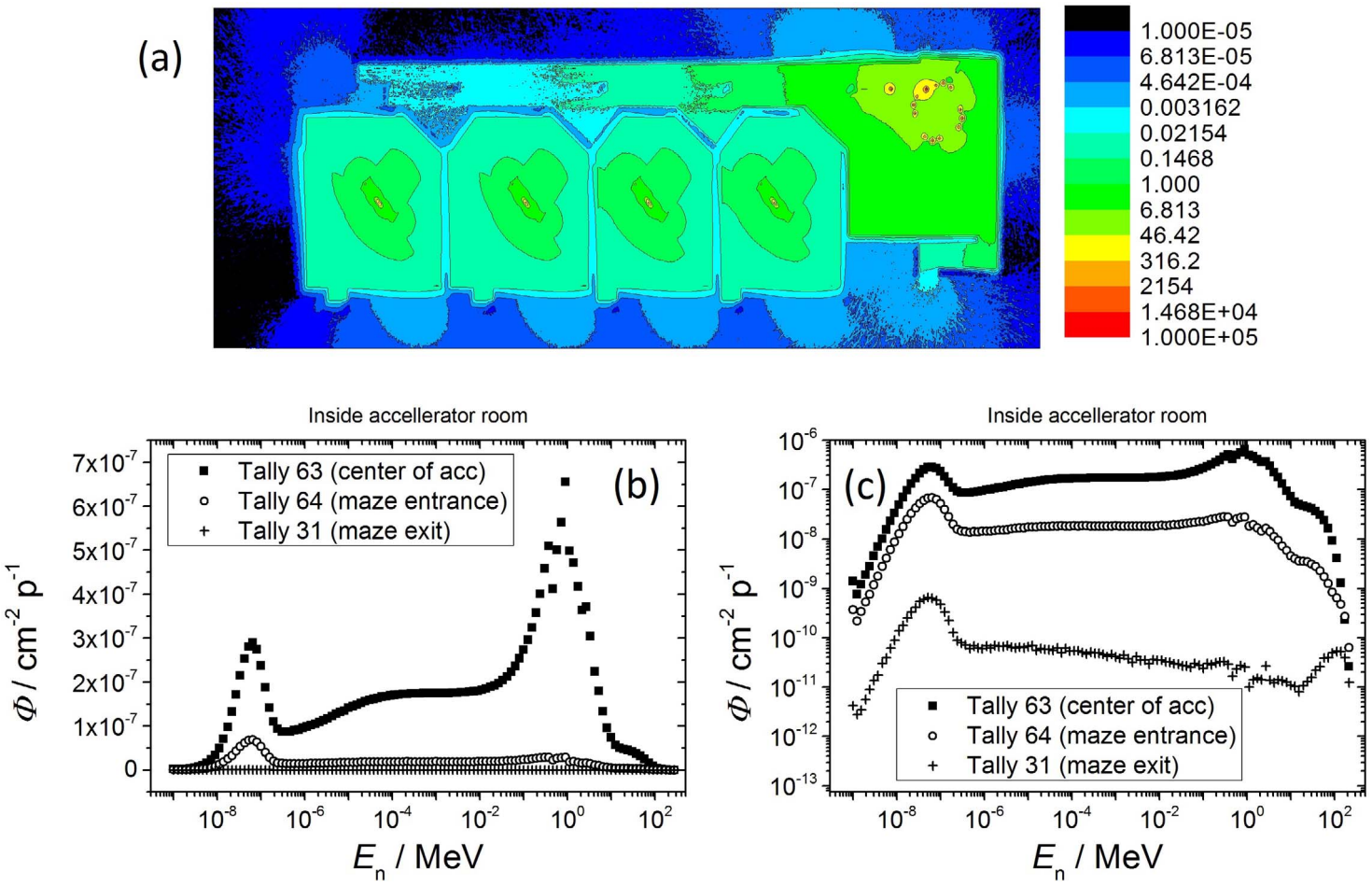

Figure 3. Panel (a) shows the 2-dimensional logarithmic plot of total neutron fluence in arbitrary units, weighted with the annual beam-loss estimates, in the isocenter plane. The lower plots show neutron spectral fluence Φ per cm^2 and source proton, p, from receptors located at the center of the accelerator, at the entrance and exit of the maze to the accelerator room in semi-log (b) and in log-log (c) plots.

into the room next door (ie, no beam in the room with the receptor). The latter data point refers to a similar boring in the wall at the end of the beam tunnel, outside of which another receptor was located. This location is the only place showing an ambient dose equivalent value close to (but still smaller than) the hourly limit of 0.02 mSv/h for members of the public. If necessary, this value could easily be decreased by sealing the hole with concrete instead of steel. Finally, the ambient dose equivalent was computed at the entrance of the air conditioner ducts on the second floor of the building. These ducts had a diameter of 40.6 cm and were embedded in all treatment room walls. Concerns these would lead to leakage and hence prohibitive neutron ambient dose equivalent values could be dismissed.

Differences in annual ambient dose equivalent based on the impact of the conduits are shown in **Figure 4c**. The values were found to be rather small in all receptor locations and did not violate the legal limits in any location.

Results of comparisons of the sliding doors versus the maze designs are given in the following paragraph. Note that only in-room irradiation conditions using the highest proton energy were used for this study. Neutron spectra located at the exit of the mazes and outside the sliding door were converted into neutron ambient dose equivalent and related to the values established with the sliding door design (see **Figure 4d**). The door on the right-hand side showed about 3.75 times enhanced neutron ambient dose equivalent values due to the fact that the door location was in line with the beam direction and the in-room wall had a thickness of 115 cm, not enough to shield the high-energy neutrons sufficiently. The maze design with the door on the left side showed neutron ambient dose equivalent values only 0.2 times that of the sliding-door design, resulting in a more efficient design in terms of shielding properties. Nevertheless, the sliding door yielded values within the annual and hourly legal limits and provided a more efficient design concerning spatial (and hence financial) aspects, and this design was considered the most appropriate for the planned facility.

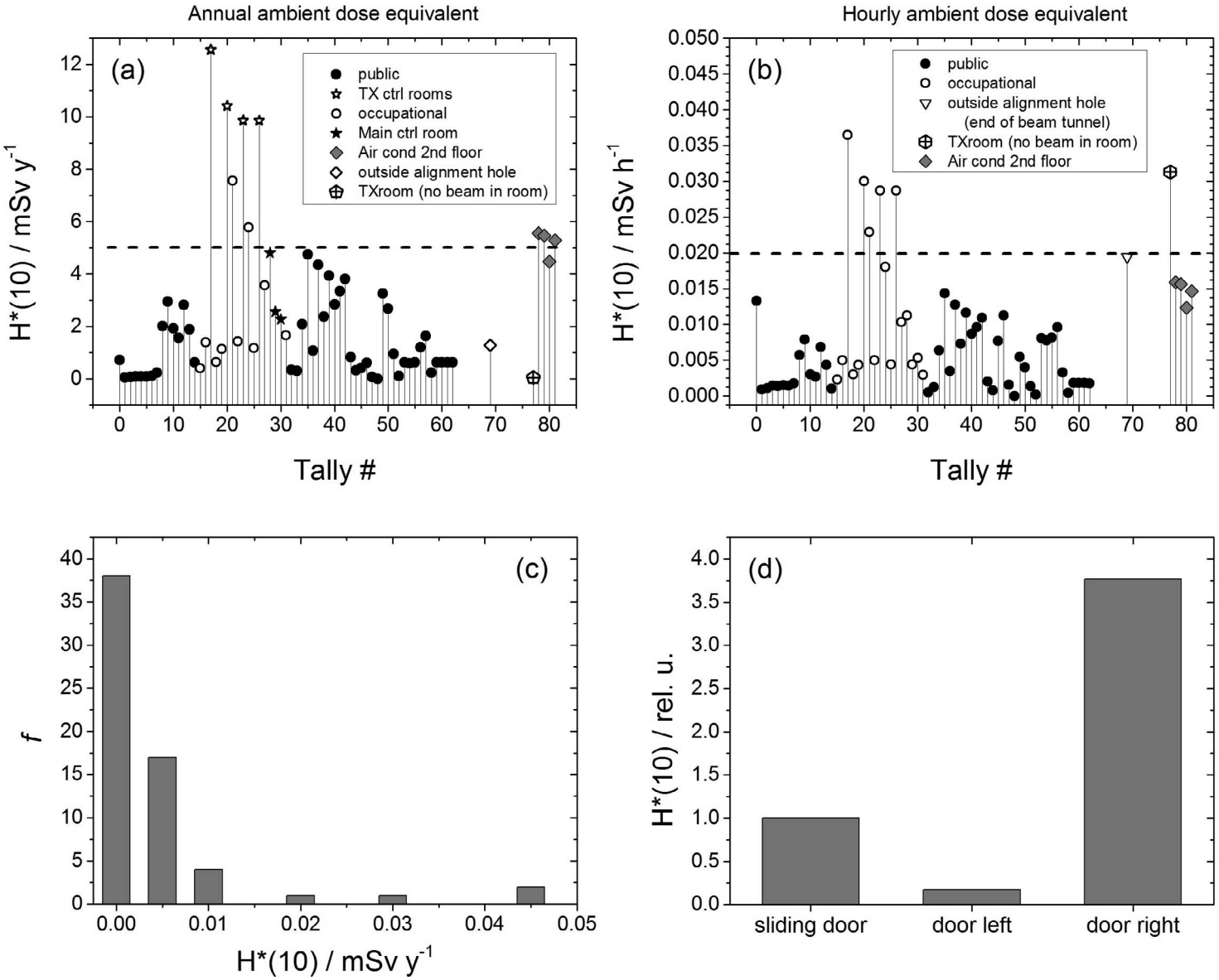

Figure 4. Ambient dose equivalent, H*(10) in units of mSv per year, based on summation over the ambient dose equivalent spectra weighted with annual (a) and hourly (b) proton loss estimates. All receptors, except the ones inside the accelerator room and inside the treatment room, are shown here. The hourly H*(10) data point for TXroom describes the value in the treatment room next to the accelerator when the beam was delivered to the treatment room next to it. Panel (c) shows the frequency *f* of the differences in annual ambient neutron dose equivalent between simulations of the complete facility with and without all the conduits in place. Panel (d) shows relative neutron ambient dose equivalent values simulated at the exit of a treatment room featuring different door designs.

Discussion and Conclusion

The simulation of a novel proton therapy facility was performed with a Monte Carlo model to evaluate the shielding properties of the concrete structure. Educated assumptions about the facility usage were applied to estimate the annual and hourly neutron ambient dose equivalent, a conservative operational quantity used in radiation protection studies. The neutron ambient dose equivalent was derived from scored neutron fluences depending on the particular type of proton interaction cross-section tables that have been applied to the simulations. Generally, the accuracy of these tables is a subject for discussion; however, published studies have shown excellent agreement and consistency with previous values and measurements in the literature [5, 6, 20, 22, 23]. Statistical and systematic uncertainties in the scored neutron fluences must be assumed to be difficult to estimate because they strongly depended on source and receptor locations, source particle energies, gantry orientations, and other factors. To mitigate such uncertainties, we applied the most conservative estimates

and assumed worst-case scenarios in all situations. In all cases the neutron ambient dose equivalent estimates were below the legal limits as defined in the Texas Code.

The facility features novel design aspects, such as straight conduits in some locations, and massive sliding concrete doors with metal plating instead of the more traditional maze design. Both design features provide economic advantages during construction and allow easier access to the treatment rooms for patients and personnel. These features were evaluated in detail and the results showed adequate shielding properties. The only value of concern may be found at an alignment hole, the end of the beam tunnel, where the simulations led to hourly neutron ambient dose equivalent values very close to the legal limit of 0.02 mSv h^{-1}. The authors recommend that this value could easily be lowered by simply filling the alignment hole with concrete instead of the temporary sealing with steel plates and steel wool. In conclusion, this work presents results computed from Monte Carlo simulations verifying the neutron shielding performance of a proton therapy facility concrete structure containing novel design features. All neutron ambient dose equivalent values, computed using worst-case usage assumptions, were below the requirements defined in the Texas Administrative Code [14].

ADDITIONAL INFORMATION AND DECLARATIONS

Conflicts of Interest: The authors have no relevant conflicts of interest to disclose.
Acknowledgments: The authors would like to thank Hitachi Ltd. for providing the blueprints of the proposed facility and detailed beam loss estimates.

References

1. Hall EJ, Kellerer AM, Friede H. Dependence on neutron energy of the OER and RBE. *Int J Radiat Oncol Biol Phys*. 1982;8: 1567–72.
2. Hall EJ. RBE and OER values as a function of neutron energy. *Eur J Cancer*. 1974;10:297–9.
3. Lai BL, Sheu RJ, Lin UT. Shielding analysis of proton therapy accelerators: a demonstration using Monte Carlo-generated source terms and attenuation lengths. *Health Phys*. 2015;108:S84–93.
4. Sunil C. Analysis of the radiation shielding of the bunker of a 230MeV proton cyclotron therapy facility; comparison of analytical and Monte Carlo techniques. *Appl Radiat Isot*. 2016;110:205–11.
5. Titt U, Newhauser WD. Neutron shielding calculations in a proton therapy facility based on Monte Carlo simulations and analytical models: criterion for selecting the method of choice. *Radiat Prot Dosimetry*. 2005;115:144–8.
6. Zheng Y, Newhauser W, Klein E, Low D. Monte Carlo simulation of the neutron spectral fluence and dose equivalent for use in shielding a proton therapy vault. *Phys Med Biol*. 2009;54:6943–57.
7. Satoh D, Maeda Y, Tameshige Y, Nakashima H, Shibata T, Endo A, Tsuda S, Sasaki M, Maekawa M, Shimizu Y, Yamazaki M, Katayose T, Niita K. Shielding study at the Fukuchi Prefectural Hospital Proton Therapy Center. *J Nucl Sci Technol*. 2012;49:1097–109.
8. Avery S, Ainsley C, Maughan R, McDonough J. Analytical shielding calculations for a proton therapy facility. *Radiat Prot Dosimetry*. 2008;131:167–79.
9. Kim JW, Kwon JW, Lee J. Design of radiation shielding for the proton therapy facility at the National Cancer Center in Korea. *Radiat Prot Dosimetry*. 2005;115:271–5.
10. Cadini F, Bolst D, Guatelli S, Beltran C, Jackson M, Rosenfeld AB. Neutron shielding for a new projected proton therapy facility: a Geant4 simulation study. *Phys Med*. 2016;32:1862–71.
11. Fan J, Luo W, Fourkal E, Lin T, Li J, Veltchev I, Ma CM. Shielding design for a laser-accelerated proton therapy system. *Phys Med Biol*. 2007;52:3913–30.
12. Prusator MT, Ahmad S, Chen Y. Shielding verification and neutron dose evaluation of the Mevion S250 proton therapy unit. *J Appl Clin Med Phys*. 2018;19:305–10.
13. Sheu RJ, Lai BL, Lin UT, Jiang SH. Source terms and attenuation lengths for estimating shielding requirements or dose analyses of proton therapy accelerators. *Health Phys*. 2013;105:128–39.
14. Texas Administrative Code §289.231. General Provisions and Standards for Protection Against Machine-Produced Radiation, Dept of State Health Services Radiation Control Program; 2004.

15. Waters LSH, J.; and McKInney, G. Los Alamos Natinal Laboratory. MCNPX version 2.5.0, 2005.
16. Seltzer S, Berger M. Evaluation of the collision stopping power of elements and compounds for electrons and positrons. *Int J Appl Radiat Isot*. 1982;33:1189–218.
17. Lorente A, Gallego E, Vega-Carrillo HR, Mendez R. Neutron shielding properties of a new high density concrete. Paper presented at: 12th International Congress of the International Radiation Protection Association; 19–24 October, 2008; Buenos Aires, Argentina. http://oa.upm.es/4596/1/INVE_MEM_2008_61569.pdf. Accessed Feb.17, 2020.
18. International Commission on Radiation Units and Measurements. *Stopping Powers and Ranges for Protons and Alpha Particles (Report 49)*. Bethesda, MD: ICRU; 1993. https://icru.org/home/reports/stopping-power-and-ranges-for-protons-and-alpha-particles-report-49. Accessed Feb.17, 2020.
19. Petoussi-Henss N, Bolch WE, Eckerman KF, Endo A, Hertel N, Hunt J, Pelliccioni M, Schlattl H, Zankl M; International Commission on Radiological Protection; International Commission on Radiation Units and Measurements. Conversion coefficients for radiological protection quantities for external radiation exposures. ICRP Publication 116. *Ann ICRP*. 2010; 40:1–257.
20. Polf JC, Newhauser WD, Titt U. Patient neutron dose equivalent exposures outside of the proton therapy treatment field. *Radiat Prot Dosimetry*. 2005;115:154–8.
21. International Commission on Radiation Units and Measurements. *Determination of Operational Dose Equivalent Quantities for Neutrons (Report 66)*. Bethesda, MD: ICRU; 2001.
22. Perez-Andujar A, Zhang R, Newhauser W. Monte Carlo and analytical model predictions of leakage neutron exposures from passively scattered proton therapy. *Med Phys*. 2013;40:121714.
23. Zheng Y, Newhauser W, Fontenot J, Taddei P, Mohan R. Monte Carlo study of neutron dose equivalent during passive scattering proton therapy. *Phys Med Biol*. 2007;52:4481–96.